The Ability of Large-Scale Ocean Models to Accept Parameterizations of Boundary Mixing, and a Description of a Refined Bulk Mixed-Layer Model

Robert Hallberg

NOAA Geophysical Fluid Dynamics Laboratory, Princeton, New Jersey – USA

Abstract. There are a number of barriers to the adoption of improved parameterizations of diapycnal mixing in large-scale ocean models. Two such barriers are discussed in detail. Ocean models often exhibit levels of spurious numerical diapycnal mixing that are so large, compared with the physical values, that parameterizing additional mixing is counterproductive, even when that additional mixing is physically well motivated. In addition, model resolution can inhibit the inclusion of observationally motivated mixing parameterizations. The remedy to the spurious diapycnal mixing lies with improved numerical algorithms or with the use of isopycnic ocean models that avoid this difficulty altogether. Selectively enhancing the resolution can greatly improve the ability of an ocean model to accept parameterizations of subgridscale physical processes. This last point is illustrated by considering the representation of dense water overflows in large-scale ocean models of several classes. It is also illustrated with a refined bulk mixed layer, in which added degrees of freedom within the mixed layer allow both resolved and parameterized shear-driven restratification, with a dramatic impact on the modeled mixed-layer depth. This refined bulk mixed layer in conjunction with an isopycnic interior model may prove to be a viable alternative approach to hybrid pressure-isopycnic coordinate models for the treatment of near-surface processes in large-scale ocean models, and it is described in detail.

Introduction

Diapycnal mixing is often depicted in large-scale ocean models in ways that seem rudimentary to people who study the physical processes that govern that mixing. For example, although the planetary boundary layer is now typically modeled with relatively sophisticated parameterizations such as KPP (*Large et al*., 1994), it is not uncommon for interior diapycnal mixing to be described in climate models by the vertically varying but flow-independent diffusivities first introduced by *Bryan and Lewis* (1979). Efforts are underway to include more realistic boundary mixing parameterizations in large-scale ocean models, but the success of this effort will be partially constrained by the suitability of the large-scale models for accommodating these parameterizations. The two substantial barriers that prevent large-scale ocean models from being able to incorporate more realistic parameterizations of diapycnal mixing—unsuitable resolution and numerical errors that can overwhelm the effect of the mixing—are discussed at length in this manuscript.

In addition to these two substantial barriers, there are a number of practical barriers to the inclusion of more realistic representations of boundary mixing processes in large-scale ocean models. The most pervasive of these is a simple lack of communication between process observationalists and climate modelers. All too often, there has been an unfortunate disconnect in the translation of process-study wisdom into large-scale ocean modeling practice. The outcome of observational process studies is typically a manuscript describing, in great detail, the phenomena at a particular time and place, or even general principles based on the kilometer-scale and smaller ocean structure, while ocean general circulation models demand globally applicable statements based on horizontal scales of tens or hundreds of kilometers. Typically the ultimate outcome of observational analysis is not cast as climate-model ready parameterizations. This disconnect has not been helped by

the fact that climate models have historically been hopelessly coarse for resolving the scales upon which many parameterizations would be based. Nor have ocean model codes traditionally been written to facilitate the exchange of parameterizations. But all of these sociological barriers can be overcome. With a concerted effort to work across subdisciplines, there is every reason to expect that great progress could be made in improving the representation of small-scale mixing processes in comprehensive large-scale ocean models.

From the perspective of climate modelers, there are several other practical considerations that severely inhibit the introduction of new parameterizations into ocean models. Foremost is the need to thoroughly understand exactly what a parameterization does and how it interacts with the rest of the climate system. Climate modelers tend to be justifiably conservative in adopting changes that might impact their ability to confidently predict how a climate model will react or might degrade the robustness of that numerical system as a whole. For example, the KPP mixed-layer parameterization of *Large et al*. (1994) is unambiguously more realistic than the ocean mixed-layer parameterizations that GFDL had used previously, and it is cast in precisely the form needed for a large-scale ocean model, but it was only in 2002 that GFDL adopted this algorithm in its primary IPCC-class coupled climate model.

Simpler parameterizations are easier to understand and implement and can qualitatively represent observational understanding. For example, the *Bryan and Lewis* (1979) vertically varying diffusivity profile does capture the sense, going back to microstructure measurements by *Gregg* (1977), that diapycnal diffusion is much higher in the abyss than in the thermocline. This qualitative description still applies to the vertical structure of diapycnal mixing, even as our knowledge of the horizontal distribution of mixing grows (*Polzin et al.*, 1997).

One of the great virtues of the Bryan and Lewis mixing parameterization is that it has essentially just four adjustable values (the thermocline diffusivity, the abyssal diffusivity, and the depth and distance over which the transition between the two occurs). Since large-scale gravity-, Kelvin-, topographic-, and Rossby-wave adjustment widely distributes the effects of locally enhanced diapycnal diffusivity (*Simmons et al*., 2003), it has been possible to tune the diffusivities to qualitatively reproduce the large-scale density structure. Such simple specifications as this have persisted in climate models, in essence, because they are difficult to qualitatively surpass in the large-scale density structures that they produce.

Ultimately, though, the fidelity of large-scale ocean models in predicting the behavior of the true ocean depends critically upon including the parameterizations that best capture our understanding of the significant processes, both in their mean effect and the sensitivity to the larger scale ocean state. The practical barriers just described can be overcome with some determination. It will be a more substantial challenge to develop ocean models that are intrinsically sufficiently adiabatic to allow the parameterizations to dominate the watermass modifications. The large-scale ocean models will also have to be constructed with resolutions that are appropriate for representing the scales of larger-scale motions upon which the parameterizations depend, while still being efficient enough to be practical for century-scale climate studies. These two challenges will be discussed in detail in the subsequent sections.

Spurious diapycnal mixing

Diapycnal mixing in the interior ocean is well known to be some 8 orders of magnitude smaller than its along-isopycnal counterpart. Even when the aspect ratio of oceanic flows (of order 10^{-3}) is taken into account, diapycnal mixing is still exceedingly weak. If model numerics lead to unintended diapycnal watermass modification that is much larger than the physically relevant mixing, even the most accurate parameterization may be of little value. In the Z-coordinate models that have traditionally been used, there are several documented sources of spurious diapycnal mixing, each of which may be of comparable magnitude to the physical diapycnal mixing in the real ocean.

Ocean models typically require explicit or implicit diffusion of tracers for numerical stability, with a horizontal projection that is of order the square of the grid-cell aspect ratio larger than the vertical projection. This can be accomplished without creating excessive diapycnal diffusion by rotating the diffusion tensor to be aligned with density surfaces (*Solomon*, 1971; *Redi*, 1982). However, if that diffusion is not rotated to be aligned with isopycnals, *Veronis* (1977) points out that it can lead to significant diapycnal diffusion. If the slope between isopycnals and the

coordinate surfaces is

$$\alpha = -\nabla_z \rho \Big/ \frac{\partial \rho}{\partial z}, \qquad (1)$$

the effective diapycnal diffusivity is given by

$$K_{D,Effective} \approx K_H \frac{1}{A} \iint \|\alpha\|^2 dA \approx O(1\ cm^2\ s^{-1}) \qquad (2)$$

where the latter order-of-magnitude estimate is based on typical horizontal diffusivities of 10^3 m^2 s^{-1}, and slopes of 10^{-3} covering 10% of the domain. As shown in Fig. 1, this estimate agrees with the diagnosed spurious diapycnal diffusivity in an idealized gyre. This diffusion clearly exceeds physical values. The same issue arises if an unrotated biharmonic diffusion operator is used (*Roberts and Marshall*, 1998). The numerical instabilities that require this diffusion can be avoided with such physically reasonable parameterizations as that of *Gent and McWilliams* (1990), and there are perfectly stable formulations for rotating the diffusion tensor to align with isopycnal surfaces (*Griffies et al.*, 1998; *Griffies* 1998). There is no excuse for using ocean models that exhibit excessive diapycnal diffusion due to an unrotated Fickian diffusion tensor.

Advective truncation errors constitute a less appreciated, but potentially equally problematic, source of spurious diapycnal watermass modifications in Z- and σ-coordinate ocean models (*Griffies et al*., 2000). Any stable tracer advection scheme leads to dispersive or diffusive truncation errors (often both), and *Griffies et al.* (2000) demonstrate how the short-term evolution of the volumetric census of watermasses in an ocean model can be used to quantify the effective levels of diapycnal diffusion.

Griffies et al. (2000) find that the diapycnal diffusion can be made acceptably small in coarse resolution models, provided that the viscosities are sufficiently large that all of the significant flow structures, especially western boundary currents, are resolved with several grid points (Fig. 2).

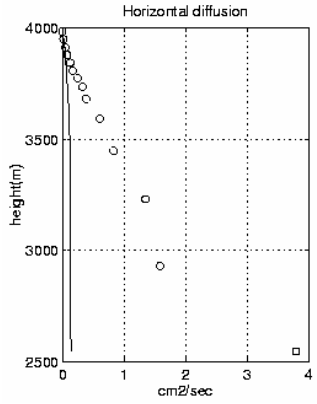

Figure 1. The effective diapycnal mixing due to an unrotated horizontal diffusion of 1000 $m^2 s^{-1}$ in an idealized gyre simulation with a Z-coordinate ocean model. This demonstration of the well-known "Veronis effect" is taken from *Griffies et al*. (2000). For reference, the diagnosed diffusivity due to a diapycnal diffusion of 10^{-5} $m^2 s^{-1}$ is also shown; geometric considerations lead to a non-constant diagnosed diffusivity. The sea surface is at the top of this plot and is labeled as a height of 4000m.

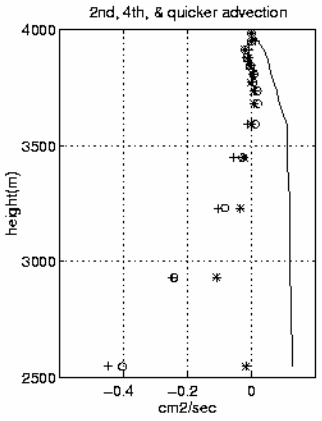

Figure 2. The effective diapycnal diffusivity due to advective truncation errors in an idealized gyre circulation with three different advection schemes, from *Griffies et al*. (2000). Centered differencing (marked with o) is a traditional choice in ocean models, while quicker (+) is the most commonly used option in MOM4. Fourth-order (*) is more accurate for well-resolved flow but can be problematic with complicated topography. In this case the viscosity is strong enough that the western boundary currents are well resolved. The line shows the diagnosed diffusivity that results from an explicit diapycnal diffusivity of 10^{-5} $m^2 s^{-1}$. Negative diffusivity is due to the dispersive creation of new watermasses. Large positive or negative diagnosed diffusivities are both undesirable.

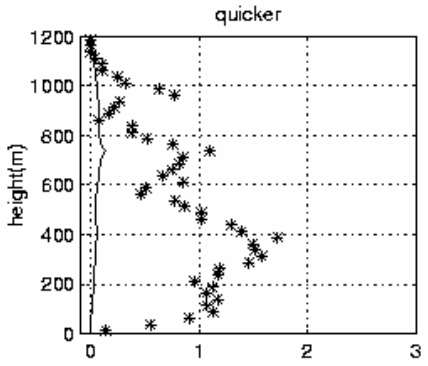

Figure 3. The effective diapycnal diffusivity due to advective truncation errors in an eddy-rich channel simulation with a Z-coordinate models, from *Griffies et al.* (2000). The cascade of variance to the grid scale ensures that there is substantial variation of density at the scales where the truncation errors become problematic. It is not yet known how to avoid spurious diapycnal diffusion of this magnitude in practical eddy-rich Z- or σ- coordinate ocean models.

In eddy-rich models, there is a cascade of variance to the smallest permitted scales. In Z- and σ-coordinate models this can lead to effective diapycnal diffusivities with magnitudes well in excess of the physical values (Fig. 3) (*Griffies et al.*, 2000). *Lee et al.* (2002) find similarly large values of spurious diapycnal diffusion in an analysis of a ¼ degree global Z-coordinate model; there is every reason to believe that this problem is widespread in the ocean models currently in use. Avoiding this unacceptably large diapycnal watermass modification is an area of active research, but it may require either suppressing the cascade of variance or using a high enough resolution to allow a separation of the scales at which the variance is absorbed from the grid scale. The cost of this unexploited higher resolution is almost certainly excessive, while important physical phenomena would be eliminated with the suppression of the eddy variability.

By construction, pure isopycnic coordinate models avoid any unparameterized watermass modifications, apart from those due to the nonlinear equation of state. This is equally true for low-resolution and eddy-rich models. All of the advective truncation errors are restricted to the isopycnal direction. If these errors are diffusive and modest, even the diapycnal transformation might be described as physically reasonable cabbeling, although the rate of the cabbeling may be controlled by numerics rather than physical constraints (Iskandarani and Chassignet, personal comm.). Apart from effects of a nonlinear equation of state, the water mass census in pure isopycnic coordinate models does not evolve without explicit diapycnal mixing.

In summary, the levels of physical diapycnal mixing in the ocean are often sufficiently weak that the spurious numerical watermass modifications in ocean models may completely mask physically consistent parameterizations. With state-of-the art numerics, acceptably adiabatic numerics exist for sufficiently laminar flows. But for eddy-rich flows most of the ocean models presently in use may not offer a practical capability for sufficiently adiabatic flows to allow physical parameterizations of mixing to control the long-term evolution of the ocean structure.

Exploiting resolution for parameterizations

Parameterizations require models to resolve the scale upon which the parameterizations depend. While this may seem obvious, it leads to very real considerations for how large-scale ocean models must be modified to accommodate the parameterization of particular processes. This will be illustrated here by considering dense water overflows.

Dense water overflows are a critical element in the formation of many of the denser water masses that fill the ocean. Typically overflows extend for up to hundreds of kilometers with dense water cross sections tens to hundreds of kilometers along the sloping bottom and tens to about a hundred meters thick. Figure 4 is an idealized illustration of an overflow. During their transit, their volume flux may increase very little or several fold due to entrainment, depending upon the properties of the flow. *Price and Baringer* (1994) provide a clear and comprehensive summary of observations and idealized models of overflows.

Overflows tend to be much thinner than the typical deep vertical grid spacing in Z-coordinate models, and they would extend diagonally between grid cells while advection is horizontal and vertical. As illustrated in Fig. 5, relying upon increased resolution to accurately represent overflows in Z-coordinate models might require vertical resolutions of order tens of meters at all depths and horizontal resolutions of order kilometers. This resolution is clearly prohibitive for many applications.

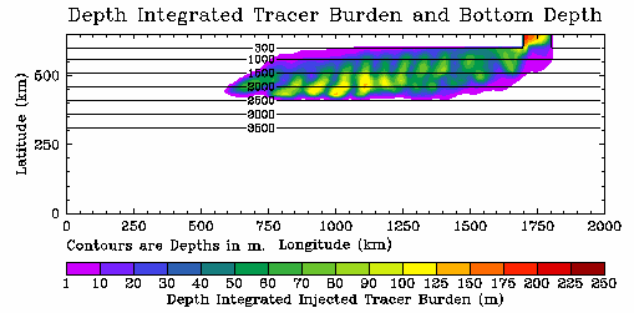

Figure 4. An idealized entraining gravity current, seen in plan view. The stratified ambient water is initially at rest, and dense water is injected at the top of a slope with the density of the deepest ambient water. The contours show the bottom depth, while the shading shows the vertically integrated burden of a tracer that is injected with concentration 1. Rotation turns the flow to the right, and strong entrainment due to a Richardson number dependent parameterization causes the plume the reach its neutral depth 1500 m above the bottom. This figure also illustrates the tendency for eddies to contribute to the downslope flow.

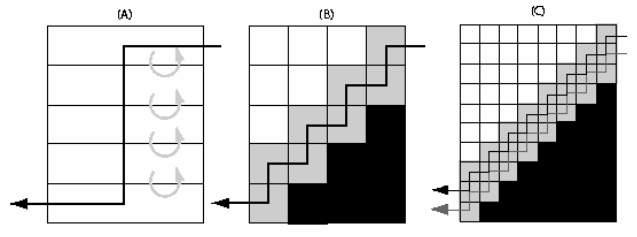

Figure 5. Schematic representation of the reduction in resolution-induced entrainment that accompanies improved resolution in Z-coordinate ocean models, adapted from *Winton et al*. (1998). When the horizontal resolution does not resolve the slope (i.e. $\Delta x << H/\alpha$, where α is the topographic slope and H is the bottom boundary layer thickness), the dense signal in the bottom layer mixes (convectively) across a number of vertical layers at each step (A). When the vertical and horizontal resolution just captures the bottom boundary layer thickness, there is still substantial mixing with ambient fluid at each step (B). It is only when $\Delta z << H$ and $\Delta x << H/\alpha$ that numerical entrainment at each step becomes negligible (C).

A more promising approach is to append bottom-following resolution to the bottom of a Z-coordinate model. The papers by *Killworth and Edwards* (1999) and *Killworth* (2003; elsewhere in this volume) describe one promising approach for representing entraining gravity currents. This additional resolution can then be used to implement a parameterization of bottom boundary layer entrainment; the thickness of this additional layer is a prognostic variable of the entrainment parameterization.

Isopycnal coordinate model representations of entraining gravity currents provide a clearer example of the distinction between having adequate resolution for a parameterization and the incorporation of the parameterization itself.

The vertical resolution in isopycnal coordinate models automatically tracks any density front, including the one at the top of a gravity current. This resolution is perfectly situated to capture all of the vertical structure of the gravity current, as is illustrated in Fig. 6a. But the very small horizontal-scale structures through which the mixing actually occurs [such as Kelvin-Helmholtz billows (e.g., *Özgökmen and Chassignet*, 2002)] are not resolved and there is very little mixing. In the absence of a suitable mixing parameterization, dense water slides down the slope essentially undiluted (Fig 6b). This, of course, differs markedly from all observations of oceanic dense water overflows (*Price and Baringer*, 1994).

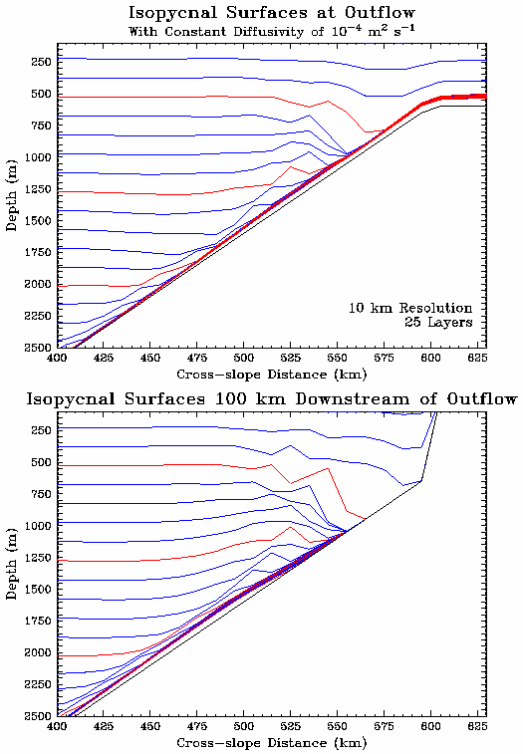

Figure 6. Cross sections showing isopycnal surfaces at the longitude of the inflow of dense water (top) and 100 km downstream. The configuration is the same as that shown in Fig. 7, but uses a constant diapycnal diffusivity of 10^{-4} m^2 s^{-1}. Without a Richardson number-dependent mixing parameterization, the densest water slides down the slope virtually undiluted.

The natural resolution of gravity currents can be used quite successfully to apply parameterizations. *Hallberg* (2000) details how the nonlinear diapycnal diffusion equation in isopycnic coordinates can be implemented implicitly for an arbitrary distribution of diffusivities. (Diapycnal diffusion is nonlinear in isopycnic coordinates because the movement of the coordinates appears as an advective term.) The relationship between the work done by mixing and diapycnal diffusivities is particularly simple to evaluate in isopycnic coordinates

$$Work = \int g\kappa d\rho = g\kappa\Delta\rho \qquad (3)$$

making a work based mixing formulation very easy to implement. Entrainment can also be parameterized directly, based upon the resolved shear Richardson number and a reinterpretation of the *Ellison and Turner* (1959) bulk Richardson number dependent parameterization (*Hallberg* 2000). Fig 7 is the counterpart of Fig. 6 when this mixing parameterization is applied. Vigorous entrainment occurs rapidly as the fluid accelerates down the slope, but essentially ceases as the plume nears its neutral depth and the Richardson number increases past the critical value, giving a plume that is qualitatively similar to many oceanic plumes. *Papadakis et al*. (2003) have applied this approach to simulations of the Mediterranean outflow, and find that the plumes with this parameterization are quite similar in watermass structure and transport to the observed outflow.

The overflows discussed here provide one particularly clear illustration of the importance of resolution in enabling parameterizations, but of course this a general consideration. The next section uses bulk mixed layers as another example of resolution-induced limitations to the physical processes that can be parameterized in large-scale ocean models.

Resolution-induced limitations to bulk mixed-layer models

The surface mixed layer is perhaps the most important part of the ocean to describe accurately for climate studies. It is through mixed-layer processes that many interior water properties are set, and the mixed layer is of leading importance in determining the sea surface temperature—the oceanic property to which the atmosphere responds most strongly.

Pressure (or depth) is the natural vertical coordinate for describing the surface mixed layer (Fig 8.). With a fine enough vertical resolution, depth coordinate models should be able to accept parameterizations of all mixed layer processes. Currently typical vertical resolutions are ~10 m in climate models, but it is an open question what resolution is globally adequate, as this resolution plays some role in determining the effective heat capacity of surface mixed layer. This is true regardless of how the mixed-layer depth is diagnosed; the finite resolution discretization of a continuous profile of temperature and salinity is inevitably affected by the location of the bottom of the well-mixed surface layer relative to a coordinate interface.

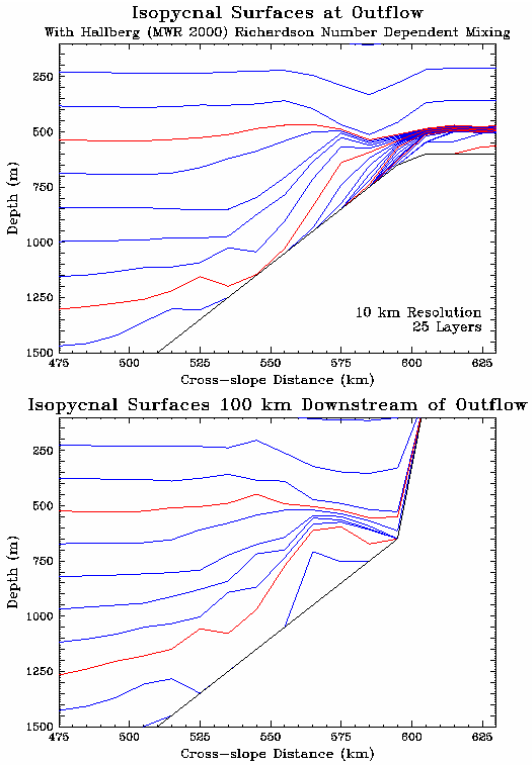

Figure 7. Cross sections showing isopycnal surfaces at the longitude of the inflow of dense water (top) and 100 km downstream. The idealized configuration is the same as that shown in Fig. 6, but uses a Richardson number dependent mixing parameterization. (Note the different axis scales between Fig. 6 and this figure. The isopycnals that rise abruptly at the coast are a plotting artifact.) The plume entrains rapidly near the inflow and achieves its neutral depth after a modest descent, similar to such plumes as the Mediterranean. The contrast with Fig. 6 is dramatic and obvious.

Density is a poor vertical coordinate for describing the vertical structure of the surface mixed layer, almost by definition. As a result, isopycnal coordinate models have traditionally been joined with bulk mixed layer models (Fig. 8). But these are not perceived as being as physically faithful to the ocean as is KPP (for example), principally because of the difficulties with depicting a detraining mixed layer, but also because of the recent emphasis of mixed layer parameterization development on that paradigm. Adding a buffer layer below the mixed layer alleviates many of the problems with detrainment. There are now substantial efforts to develop density-pressure hybrid coordinate models (e.g., *Bleck*, 2002), largely to enable the use of an isopycnal interior with a KPP-style mixed layer parameterization.

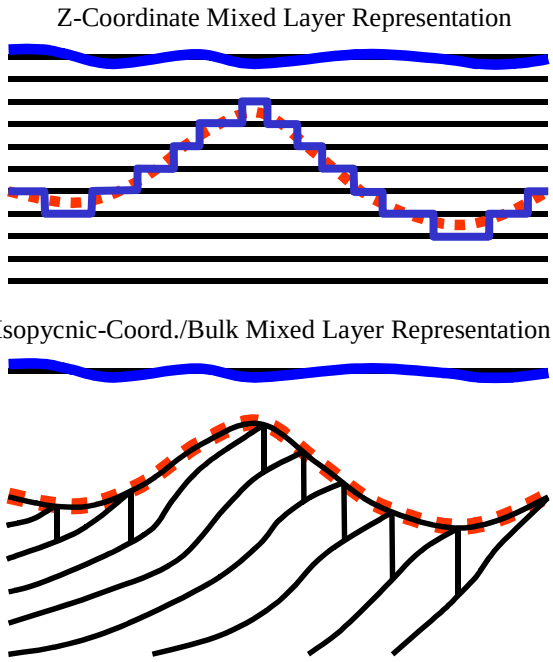

Figure 8. Schematic representation of the surface mixed layer with Z-coordinate ocean models (top) and isopycnic coordinate models coupled with bulk mixed layer models (bottom). The true mixed-layer depth is shown with the dotted red line. In a Z-coordinate model, the effective mixed-layer depth is effectively partially quantized to coincide with the coordinate surfaces (the blocky blue line in the top panel). With a bulk mixed-layer model, the mixed-layer depth is a continuously varying prognostic variable, but there is no resolution of structure within the mixed layer and the coupling with the interior must be treated carefully, perhaps with a buffer layer that occupies the triangular areas between the mixed layer and interior in the lower panel.

There may be drawbacks to the hybrid approach, including, possibly, excessive diapycnal diffusion in the pressure coordinate region (Shan Sun, personal comm.). It may be worth considering whether the bulk mixed-layer representation might not be made more competitive with the KPP approach. Although a bulk mixed layer might not ultimately prove to be the optimal approach, it is worthwhile to fully explore each of the potentially viable options for large-scale ocean models.

Observations of the surface planetary layer reveal a number of important qualitative properties. These are well illustrated in Figs. 9 and 10. Planetary boundary layers do tend to be well mixed in properties such as temperature. Note that the temperature curves in Fig. 9 from 0 to 75 m depth are nearly indistinguishable. Momentum, however, is not so well mixed in the boundary, giving Ekman spirals with enough temporal averaging (Fig. 10). The other instructive property is that restratification can occur very quickly after violent mixing events (examples of such mixing events occur on 1/1/94, 1/6/94, 1/15–1/18/94, and 2/13-2/16/94 in Fig. 9). These restratification events do not appear to be due to mesoscale eddies that penetrate below the mixed layer.

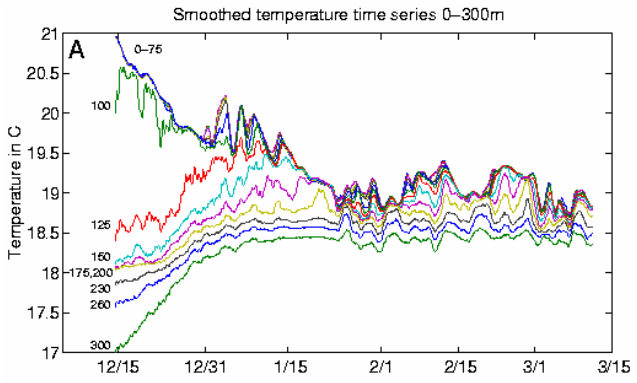

Figure 9. Near-surface temporal evolution of potential temperature at 12 depths in the ASREX III study (*Galbraith et al*., 1996). This time series has been filtered to remove variability of less than one day. ASREX was conducted at 34N, 70W, in the North Atlantic subtropical gyre. This unpublished figure is provided courtesy of Anand Gnanadesikan.

There are a number of important processes for determining the mixed-layer depth. An accurate mixed layer parameterization would probably have to include all of the following processes:

- Wind stirring-driven entrainment
- Free convective deepening
- Overshooting convective plumes
- Buoyancy-forced retreat to the Monin-Obukhov depth
- Penetrating shortwave radiation
- Vertical decay of turbulent kinetic energy
- Conversion of large-scale shears to small-scale turbulence (probably via Richardson number criteria)
- Restratification due to ageostrophic shears in the mixed layer

Of these processes, it is only the latter that clearly cannot be represented with a single-layer bulk mixed layer, but this process is clearly important from observation such as that depicted in Figs. 9 and 10.

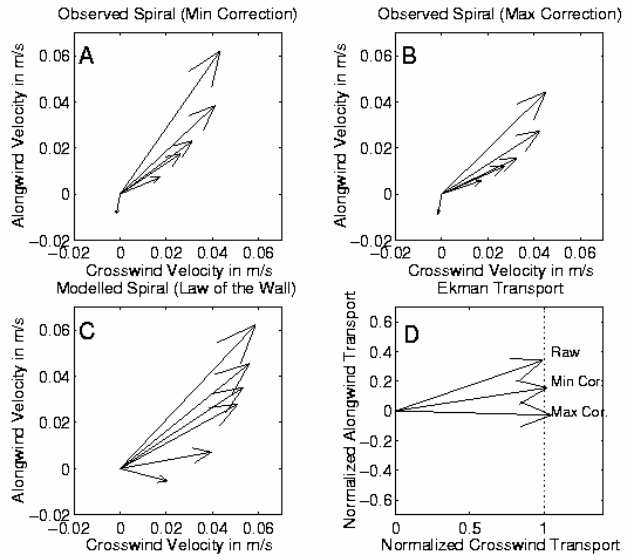

Figure 10. Near-surface time-mean velocities, relative to the flow at 300 m and rotated following the wind stress, at depths of 5, 10, 15, 20, 50, and 150 m from ASREX, during a period (1/15-1/18/94) when the mixed layer was always deeper than 150 m. These velocities exhibit a vertical structure (panels A and B) and transport (panel D) highly reminiscent of an Ekman spiral (panel C). In panels A and B, two different corrections for buoy motion biases have been applied. This unpublished figure is provided courtesy of Anand Gnanadesikan.

The nature of several of the ageostrophic restratification processes can be illustrated by considering the turbulent kinetic energy (TKE) balance equation of the surface mixed layer. The following TKE balance equation (divided by a mean density) follows *Oberhuber* (1993). Apart from folding the dissipation terms into the source terms and the inclusion of the horizontal advective restratification, it is fairly standard.

$$\underbrace{w_E \frac{h}{2} g'}_{S_{Ent}} - \underbrace{w_E Ri_{\mathrm{Crit}} \|\Delta u\|^2}_{S_{Shear}} = \underbrace{m_0 m_1 u^{*3}}_{S_{Wind}} + \underbrace{\frac{h}{2} m_2 \left\{ B - B_{\mathrm{PenSW}} \left[\frac{2}{\lambda h} \left(1 - e^{-\lambda h} \right) - e^{-\lambda h} \right] \right\}}_{S_{Buoy}} + \underbrace{m_3 \int_{-h}^{0} \frac{g}{\rho_0} \dot{\rho}_{\mathrm{Advective}} \left(z + \frac{h}{2} \right) dz}_{S_{\mathrm{Adv}}} \qquad (4)$$

where w_E is the rate of mixed layer deepening, h is the mixed-layer depth, g' is the reduced gravity across the base of the mixed layer, Ri_{Crit} is a critical bulk Richardson number, $\|\Delta u\|$ is the velocity difference between the mixed layer and the water beneath it, B is buoyancy forcing, B_{PenSW} is the buoyancy forcing due to the penetrating component of the shortwave radiation, λ is the extinction rate of the penetrating shortwave radiation, $u^* = \sqrt{\tau / \rho_0}$ is the friction velocity due to the wind stress, and $\dot{\rho}_{\mathrm{Advective}}$ is the advective density tendency relative to the vertical mean tendency. The nomenclature here follows a number of previous papers, such as the review paper of *Niiler and Kraus* (1977).

Equation (4) is the appropriate TKE equation, assuming that the thermodynamic properties are well mixed within the mixed layer, that these properties may be quasi-discontinuous across the base of the mixed layer, and that the rate at which the turbulent kinetic energy changes is small compared with the sources and sinks, so that an instantaneous balance effectively holds (*Niiler and Kraus*, 1977). Most of the terms in (4) can be derived from elementary energy considerations. S_{Ent} is the work required to mix denser water from below the base of the mixed layer up through the mixed layer. S_{Shear} is the mean kinetic energy released by homogenizing the horizontal velocity of the entrained fluid with the fluid within the mixed layer. (These shears are often due to inertial oscillations.) S_{Wind} is the TKE imparted by wind work (much of this due to surface gravity wave breaking); work is a force times a velocity, hence the dependence on $u^{*3} = u^* \tau / \rho_0$. S_{Buoy} is the work required to

mix the buoyancy forcing throughout the mixed layer from the surface (or wherever the shortwave radiation is absorbed). The final term, S_{Adv}, is the work required to mix against advective tendencies to restratify or destabilize the mixed layer, and it is omitted in purely one-dimensional mixed layer formulations. Density in (4) is described as though the ocean had a linear, incompressible equation of state; in actual model implementations, these simplifications would not be made. The energy loss from the radiation of internal waves into the ocean interior is omitted in (4).

In addition, the various m_n terms generically represent the vertical decay of turbulence. *Oberhuber* (1993) suggests that this decay might be parameterized with exponentials as

$$m_1 = \exp(-h / h_{\text{Mech}}) \tag{5}$$

$$m_2 = \begin{cases} \exp\left(-h / h_{\text{Mech}}\right) \text{ for } \left(S_{Buoy} < 0\right) \\ \exp\left(-h / h_{\text{Conv}}\right) \text{ otherwise} \end{cases} \tag{6}$$

perhaps using the plausible values

$$m_0 = 1.25 \quad Ri_{Crit} = 0.5 \quad h_{\text{Mech}} = \frac{0.4u^*}{f} \; h_{\text{Conv}} = \frac{2u^*}{f} \tag{7}$$

determined as a best fit to observations by *Oberhuber* (1993). The critical Richardson number here says that half the released energy from homogenizing mean flows goes into driving turbulence; *Price et al*. (1986) would use a value of 0.65. For consistency, if it assumed that the contribution to S_{Adv} is uniformly distributed over the mixed layer then

$$m_3 = 6\frac{1 - h\gamma + h^2\gamma^2/2 - \exp(-h\gamma)}{h^3\gamma^3} \tag{8}$$

where $\gamma = \begin{cases} 1/h_{\text{Mech}} & \text{for } S_{\text{Adv}} < 0 \\ 1/h_{\text{Conv}} & \text{otherwise} \end{cases}$. Eq. (8) has asymptotic limits of 1 and $3/h\gamma$.

When a negative entrainment is indicated, the mixed layer detrains to the Monin-Obukhov depth, h_{MO}, determined by solving

$$\frac{h_{MO}}{2} m_2 \left(B - B_{\text{PenSW}} \left\{ \frac{2}{\lambda h_{MO}} \left[1 - \exp(-\lambda h_{MO})\right] - \exp(-\lambda h_{MO}) \right\} \right) \tag{9}$$
$$+ m_0 m_1 u^{*3} + m_3 \int_{-h_{MO}}^{0} \frac{g}{\rho_0} \dot{\rho}_{\text{Advective}} \left(z + \frac{h_{MO}}{2} \right) dz = 0$$

In essence, the Monin-Obukhov depth is the depth to which the wind stirring is able to mix the density anomaly due to the surface buoyancy source. The water below this depth remains at the previous, higher density.

There are several possible sources for the advective restratification. To the extent that density is vertically well mixed through the mixed layer, the advective restratification source of mixed-layer potential energy in the TKE budget is

$$\begin{aligned} S_{\text{Adv}} &= -\int_{-h}^{0} \frac{g}{\rho_0} (\vec{u} \cdot \nabla \rho) \left(z + \frac{h}{2} \right) dz \\ &\approx -\frac{g}{\rho_0} (\nabla \rho) \cdot \int_{-h}^{0} (\vec{u} - \bar{u}) \left(z + \frac{h}{2} \right) dz \end{aligned} \quad . \tag{10}$$

Mixed-layer potential energy (MLPE) is the potential energy that can be released by thoroughly mixing convective adjustment or (if negative) the potential energy deficit that must be balanced to homogenize density through the depth of the mixed layer. From (10), it can be seen that geostrophic advection in a mixed layer with vertically homogenous density does not change the mixed layer stratification, since

$$\begin{aligned} &\frac{\partial}{\partial z} u_{\text{Geostrophic}} = -\frac{g}{f\rho_0} \hat{k} \times \nabla_H \rho \\ &\Rightarrow (\nabla_H \rho) \cdot (\vec{u} - \bar{u})_{\text{Geostrophic}} = 0 \end{aligned} \tag{11}$$

Any ageostrophic flows, though, can lead to stratification sources.

Ekman transport can be a significant source or sink of mixed layer MLPE (*Rodhe*, 1991). If the down-density gradient portion of the Ekman transport,

$$T = \left(-\hat{k} \times \vec{\tau} / f\rho_0 \right) \cdot \frac{\nabla \rho}{\|\nabla \rho\|} \tag{12}$$

is approximated as decaying linearly over a depth $\delta < h$, then the MLPE source becomes

$$\begin{aligned} S_{\text{Ekman}} &= -\int_{-h}^{0} \frac{g}{\rho_0} (\vec{u} \cdot \nabla \rho) \left(z + \frac{h}{2} \right) dz \\ &= \frac{g}{\rho_0} \|\nabla \rho\| \int_{-\delta}^{0} \frac{2T(z+\delta)}{\delta^2} \left(z + \frac{h}{2} \right) dz \\ &= \frac{g}{2\rho_0} \|\nabla \rho\| T\left(h - \frac{2\delta}{3} \right) \equiv M^2 T \left(\frac{h}{2} - \frac{\delta}{3} \right) \end{aligned} \quad . \tag{13}$$

Different profiles for the Ekman transport will change the MLPE source in detail, but not qualitatively. The Ekman-driven restratification is captured quite naturally in a model that vertically resolves these velocity shears and has the correct vertical stress (or viscosity) profile. Since the strength of this

term varies linearly with the down-transport magnitude of the horizontal density gradient, it should be described fairly well even at relatively coarse horizontal resolutions. But of course with a traditional bulk mixed layer, the Ekman mixed layer restratification is simply missing!

Viscous restratification is a significant, persistent sink of MLPE. Without vertical mixing of momentum, the mixed-layer velocities would develop thermal wind shears. If the velocity is mixed at a finite rate, sheared flows with a component down the density gradient in the sense to release potential energy. *Young* (1994) shows that if the mixed layer velocity tends to be homogenized with a timescale of $1/(\mu f)$ the inertially adjusted mixed layer velocities at leading order are

$$\vec{u} = \bar{u} - \frac{1}{1+\mu^2}\frac{g}{f\rho_0}(z+\frac{h}{2})\left(\hat{k}\times\nabla\rho - \mu\nabla\rho\right) \quad (14)$$

Ferrari and Young (1997) show that essentially equivalent downgradient flows develop whether the momentum mixing is steady or episodic. The MLPE sink due to the viscous stresses acting on the thermal wind shears in the mixed layer is:

$$\begin{aligned} S_{\text{Viscous}} &= -\int_{-h}^{0}\frac{g}{\rho_0}(\vec{u}\cdot\nabla\rho)(z+h/2)dz \\ &= -\frac{\mu}{1+\mu^2}\frac{g^2}{\rho_0^2 f}\|\nabla\rho\|^2\int_{-h}^{0}(z+h/2)^2 dz \\ &= -\frac{\mu}{1+\mu^2}\frac{g^2}{\rho_0^2 f}\|\nabla\rho\|^2\frac{h^3}{12} \equiv -\frac{\mu}{1+\mu^2}\frac{M^4h^3}{12f} \end{aligned} \quad (15)$$

Here it is worth noting that $|\mu| = h_{Ekman}/h = O(1)$, or $\mu = u^*/hf = O(1)$. This expression has a strong dependency on the mixed-layer depth (it is at least quadratic, even when the mixed layer is much deeper than the Ekman depth), and it is always negative. This term provides a strong constraint on how deep the mixed layer can become in the presence of horizontal density gradients. A consequence of viscous restratification is that horizontal temperature and salinity gradients should compensate in the mixed layer (*Ferrari and Young*, 1997), something that is in fact observed to occur on horizontal scales ranging from 20 m to 10 km (*Rudnick and Ferrari*, 1999; *Ferrari and Rudnick* 2000). As with the Ekman-driven restratification, the viscous restratification is excluded from traditional bulk mixed layer models.

The quadratic dependence on the horizontal density gradients in (15) is also quite significant as it means that this term will be systematically underestimated. The spatial mean square of the density gradient may be much larger than the square of the spatial mean density gradient if the dominant scales of variability are not resolved. Given the preponderance of fronts in the ocean, these dominant scales may be of order kilometers to tens of kilometers (e.g. *Weller*, 1991). At the typical resolutions of most ocean models, the restratification due to the unresolved scales will require parameterization to capture fully.

In addition, baroclinic eddies can cause mixed layer restratification, both through ageostrophic advection (*Nurser and Zhang*, 2000) and by straining the horizontal density gradients and consequently enhancing the viscous restratification.

Advective restratification of the mixed layer stems from several processes that are locally important for determining the mixed-layer depth. These processes are excluded by construction from traditional bulk mixed layer models. Nor is it clear that these processes can be parameterized in a straightforward way. Instead, selective addition of resolution to the mixed layer may substantially increase the viability of bulk mixed layer parameterizations in large-scale ocean models.

A refined bulk mixed-layer model

Bulk mixed layers work very naturally with isopycnic coordinate ocean models. They offer a clear transition between a thoroughly mixed planetary boundary layer and a nearly adiabatic ocean interior. There is a strong tradition of this combination, as exemplified by *Bleck et al*. (1989) and *Oberhuber* (1993). Many of the difficulties with matching water detrained from the mixed layer are avoided by using a buffer layer to mediate the return of that water to the isopycnic interior (*Murtugudde et al*., 1995; *Thompson et al*., 2002). But because bulk mixed layers do not permit velocity shears, they omit several potentially important processes, as described above.

A modification to the traditional bulk mixed layers, in which sublayers are added to permit resolution of velocity shears and of restratification, is described in this section. Velocity is homogenized within the mixed layer at a finite rate because the homogenization rate is not guaranteed to be short compared with

the inertial period. By contrast, density and advected scalars are assumed to be rapidly homogenized within the mixed layer, although advection is explicitly permitted to restratify the mixed layer to introduce the advective MLPE sink described in the previous section. After the mixed layer is applied, each of the sublayers has the same temperature and salinity, although it would be straightforward to apply a finite mixing rate, as for velocity. The purpose of this section is to illustrate how bulk mixed layer formulations can be revised to enable the introduction of the vertical resolution that is needed to permit parameterizations of the effects of mixed layer shears.

Adding resolution requires a change to the solution technique from the traditional approach, so that the results of a single-column model are unaffected by adding the resolution to the mixed layer. Traditionally, the mixed-layer depth is adjusted essentially as described in the previous section, usually assuming that entrainment is weak so that the various exponential terms in (4) are calculated based on the mixed-layer thickness at the start of a time step. If this approach were applied with multiple sublayers, the exponential terms would be most appropriately calculated at the interfaces between sublayers and the solution would be a clear function of the number of sublayers, especially when there is penetrating shortwave radiation.

Instead, the mixed-layer depth is determined from an integral TKE equation, starting from the surface, and integrated in time over a time step. The assumption that salinity and potential temperature are constant through each of the sublayers after advection is not made. The new mixed-layer depth is determined from the following steps:

• Advection restratifies the mixed layer. This may not really a part of the mixed-layer parameterization, per se, if it is the resolved velocities that drive the restratification. Within the mixed layer itself, the prescription for the vertical viscosity may be of particular importance for determining the extent of the Ekman or shear-driven restratification. In the example in the next section, velocity within the mixed layer is vertically mixed with the viscosity $0.4u^*H_{\mathrm{ML}}$. (The 0.4 here is Von Karmen's constant.) While this is a plausible placeholder specification, it needs to be evaluated carefully against both observations and large-eddy simulations.

• The mixed layer undergoes convective adjustment, saving the released potential energy to drive further mixing. In equations, the depth h_{CA} is found such that

$$\rho(-h_{CA}) = 1/h_{CA}\int_{-h_{CA}}^{0}\rho(z)dz\,, \tag{16}$$

while the released potential energy is

$$\Delta PE_{CA} = \frac{g}{2\rho_0}\int_{-h_{CA}}^{0}\left[\int_z^0\rho(z')dz' - z\rho(z)\right]dz \tag{17}$$

at this point, the density profile is

$$\hat{\rho}(z) = \begin{cases}\rho(-h_{CA}) & \text{for } z > -h_{CA}\\ \rho(z) & \text{for } z \le -h_{CA}\end{cases} \tag{18}$$

with equivalent profiles of potential temperature and salinity.

• Surface heating, cooling, evaporation, and precipitation are applied. If there is net evaporation, the salt is left in the reforming mixed layer. The sea surface height (that had previously been at z=0) becomes $\eta = (P-E)\Delta t$, while a delta-function of salinity, temperature, and density is (temporarily) retained at the new surface if there is net evaporation. That is, using a new vertical coordinate $\tilde{z} = z - \eta$, if there is net precipitation (i.e. $\eta > 0$), the profiles of potential temperature, and salinity become

$$\tilde{\theta}(\tilde{z}) = \begin{cases}\hat{\theta}(0) + \dfrac{Q\Delta t}{\rho_0 c_p \eta} + \dfrac{Q_{\mathrm{Pen}}\Delta t\lambda}{\rho_0 c_p}e^{\lambda z} & \text{for } \tilde{z} \ge -\eta\\ \hat{\theta}(z = \tilde{z} + \eta) + \dfrac{Q_{\mathrm{Pen}}\Delta t\lambda}{\rho_0 c_p}e^{\lambda z} & \text{for } \tilde{z} < -\eta\end{cases} \tag{19}$$

where Q includes all of the surface heating terms except for the penetrating component of shortwave radiation, Q_{Pen}, and

$$\tilde{S}(\tilde{z}) = \begin{cases}0 & \text{for } \tilde{z} \ge -\eta\\ \hat{S}(z = \tilde{z} + \eta) & \text{for } \tilde{z} < -\eta\end{cases}. \tag{20}$$

If there is net evaporation, these profiles become

$$\tilde{\theta}(\tilde{z}) = \hat{\theta}(z = \tilde{z} + \eta) + \frac{Q\Delta t}{\rho_0 c_p}\delta(\tilde{z}) + \frac{Q_{\mathrm{Pen}}\Delta t\lambda}{\rho_0 c_p}e^{\lambda z} \tag{21}$$

and

$$\tilde{S}(\tilde{z}) = \hat{S}(z = \tilde{z} + \eta) + \delta(\tilde{z})\int_{\eta}^{0}S(z)dz\,. \tag{22}$$

In either case, there is obviously a problem using these profiles of potential temperature and salinity in the nonlinear equation of state to calculate a potential density profile. Instead, the equation of state can be

linearized about the previous surface temperature and salinity in the delta function or above the previous sea surface, giving the new potential density profile

$$\rho(\tilde{z}) = \begin{cases} \hat{\rho}(0) + \dfrac{\partial \rho}{\partial \theta}(\tilde{\theta} - \hat{\theta}(0)) & \\ \quad + \dfrac{\partial \rho}{\partial S}(\tilde{S} - \hat{S}(0)) & \text{for } \tilde{z} \geq \min(0, -\eta) \\ \hat{\rho}(z = \tilde{z} + \eta) & \text{for } \tilde{z} < \min(0, -\eta) \end{cases} \quad (23)$$

Potential temperature and salinity are the variables that are conserved, and the equation of state is ultimately used to calculate the density, but this pseudo-potential density referenced to the surface would be used as the "MLPE currency" in the TKE balance equations. Thermobaricity could, of course, be accounted for, but this adds complexity beyond what is described here.

• The mixed layer entrains down to the depth of free convection. With penetrating shortwave radiation the temperature varies within each layer, so the depth of free convection with the layer is calculated iteratively using Newton's method once the layer containing the depth of free convection is found. If there is no shortwave radiation at a point the depth of free convection occurs at an interface between layers. The depth of free convection is determined by solving for the depth h_{FC} in

$$\tilde{\rho}(-h_{FC}) = \frac{1}{h_{FC}} \int_{-h_{FC}}^{0} \tilde{\rho}(z) dz \,, \quad (24)$$

while the available potential energy released by the free convection is

$$\Delta PE_{FC} = \frac{g}{2\rho_0} \int_{-h_{FC}}^{0} \left[\int_z^0 \rho(z') dz' - z\rho(z) \right] dz \quad (25)$$

• The new mixed-layer depth is determined by solving for the depth where all available TKE is used. First, the TKE available at the depth of free convection is determined from

$$\begin{aligned} TKE_{FC} = {} & m_0 \exp(-h_{FC} / h_{\text{Mech}}) u^{*3} \\ & + \exp(-h_{FC} / h_{Conv})(\Delta PE_{CA} + \Delta PE_{FC}) \end{aligned} \,. \quad (26)$$

This is really the first point at which the parameterization of physical processes, the sources of energy driving the mixing and the dissipative TKE sink, enters. The specific example in (26) and (27) below follows *Oberhuber* (1993), but a wide variety of other models for energy sources or sinks could be used instead. There is one significant term that is effectively missing in (26) that was present in (4), S_{Shear}, the source of TKE from homogenizing the mean velocities. Treating this term consistently is complicated by the assumption here that momentum is not immediately homogenized. It is demonstrably important for time scales of order half the inertial period (*Pollard et al*., 1973), but might be lumped in with the wind source of TKE on longer timescales (*Gaspar*, 1988). The new mixed-layer depth H is found by solving

$$\begin{aligned} 0 = {} & TKE_{FC} \exp\left(- \frac{H - h_{FC}}{h_{Mech}} \right) \\ & + \frac{g}{2\rho_0} \int_{-H}^{-h_{FC}} \left\{ \exp\left(- \frac{H + z}{h_{Mech}} \right) \left[\int_z^0 \tilde{\rho}(z') dz' - z\tilde{\rho}(z) \right] \right\} dz \end{aligned} \quad (27)$$

Here the exponential decay in the second term, TKE conversion to potential energy, reflects the fact that once a portion of the TKE has been consumed, it is no longer available to decay deeper in the water column. The full nonlinear equation (27) for this budget can be solved for the mixed layer with a few iterations of Newton's method to within a tolerance of order angstroms.

• Any fluid that is deeper than the new mixed-layer depth that had previously been in the mixed layer is detrained into a variable density buffer layer. Up until this point, there is no distinction in the calculations between the mixed layer sublayers and interior fluid.

• The fluid within the new mixed layer is divided among the sublayers. Tracer concentrations within the sublayers are set to the average over the mixed-layer depth, while momentum is advected between sublayers and mixed vertically within the mixed layer with a velocity u*.

With this prescription the mixed layer transparently accounts for advective restratification or advection induced penetrating convection. Detrainment up to the Monin-Obukhov depth is expressed here as a mixed layer that does not reentrain to its previous depth. In essence, this strategy includes all of the processes included in the *Oberhuber* (1993) mixed layer scheme. While it does not directly include either shear or bulk Richardson number criteria (as with *Price et al*. (1986)), these could be folded into the TKE budget. For example shear Richardson number driven entrainment is identified as important by *Chen et al.*, (1994), and has been implemented in HIM using the same interior diapycnal mixing parameterization (*Hallberg*, 2000) as is used to cap-

ture the gravity current entrainment described earlier. The exposition here is not intended to describe a novel, comprehensive mixed-layer parameterization but to illustrate an extension to existing bulk mixed layers (many of which have been tuned to agree with observations in locations with weak horizontal influences) to permit inclusion of the advective MLPE sources. *Oberhuber's* (1993) formulation is used here as a working prototype and as the form that has been used in the HIM examples in the next section.

As an aside, although the refined bulk mixed layer presented here has not included any new physical processes apart from the shear-driven restratification, it also offers other prospects for extensions. For example, the added resolution might be used to capture the diurnal cycle of the mixed layer, with some of the lower sublayers remaining in the deep nighttime mixed layer even as shallower layers follow the shallow daytime mixed layer, and detrainment into the buffer layer occurring only for fluid that has not actively been mixed with the surface for several days. Alternately, the resolution within the mixed layer might be used to capture the vertical structure of biogeochemical quantities that are not well mixed because they evolve over short timescales. Both of these examples are enabled by the fact that this mixed layer approach gives the same response to purely column processes (i.e. for horizontally invariant situations) for any number of mixed layer sublayers.

Resolved and parameterized shear-driven, mixed-layer restratification

By adding vertical resolution to the bulk mixed layer, there is a prospect that advective restratification might be explicitly resolved. The advective restratification or destabilization due to Ekman transport should be captured adequately even with a relatively coarse horizontal resolution. As described previously, the impact of viscous restratification on the mixed-layer depth scales with the square of the horizontal density gradient. The effectiveness of shear restratification will be a strong function of horizontal resolution up to the point where almost all of the horizontal density gradients are well resolved. These two processes provide contrasting examples of a physical process that is directly captured with adequate resolution and one in which the additional resolution enables parameterization.

An example of this is provided in Figs. 11 and 12, which are from an eddy-permitting simulation of the Southern Hemisphere using the Hallberg Isopycnal Model (HIM) (*Hallberg and Rhines*, 1996). Without mixed layer shears, the mixed layer is much deeper than is observed, although this particular simulation is not directly comparable with the observations of any one season. (This simulation has no temporal forcing variations; hysteresis in the TKE budget would lead to an equilibrium mixed-layer depth even without mixed layer shears if the forcing were cyclic.) Dividing the bulk mixed layer into two sublayers permits Ekman-driven restratification (or destabilization) and some degree of viscous restratification. The mixed layer is modestly shallower than without the shears. In regions of westerly winds (as in much of the Southern Ocean), the Ekman transport tends to destabilize the mixed layer. In the Southern Ocean, the persistent viscous restratification does lead to a shallower mixed layer, despite the tendency from the Ekman transport.

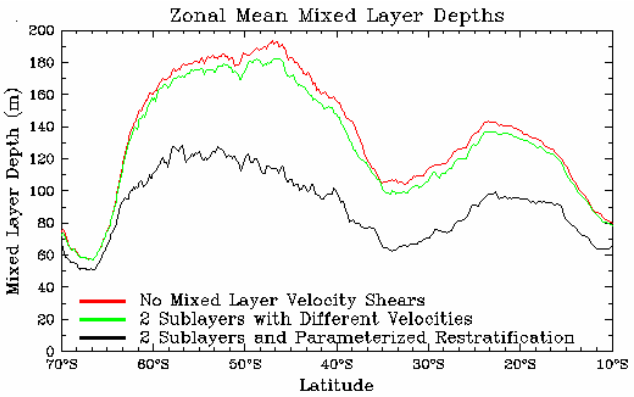

Figure 11. Zonal mean mixed-layer depth in an eddy-permitting Southern Hemisphere simulation with three different treatments of the mixed layer velocities. All three have been run 100 days from the same, well-equilibrated simulation using 2 sublayers and the parameterized restratification. The mixed-layer depths increase further over time, especially with no mixed layer shears. With resolution of mixed-layer shears there is a modest decrease in the mixed-layer depth due to both viscous and Ekman restratification. The placeholder parameterization described in the text sets a strong limit on the zonal mean mixed-layer depth.

The horizontal resolution of this simulation (20 km at 44 S) is not adequate to resolve all of the scales upon which mixed-layer density varies. Since the shear restratification scales with the area-mean square of the horizontal density gradients, there are

unresolved scales whose effects should probably be parameterized. The right way to do this is probably to use the resolved horizontal density gradient and an estimate of the spectral shape of horizontal density gradients to infer the effect of the unresolved scales. Unfortunately, this author is unaware of a mature theory along these lines. Instead, a plausible placeholder parameterization is used to evaluate the potential for shear restratification to influence the mixed-layer depth. Rather than directly estimating the subgridscale gradients, it might be assumed that the resolved horizontal gradients can be used to estimate a vaguely plausible viscous overturning circulation within the mixed layer. The maximum downgradient velocities occur when the velocity is homogenized with a timescale of (1/*f*) (Young, 1994). This leads to a zero-mean restratifying velocity profile within the mixed layer

$$\vec{u}_{RS} = \frac{1}{2}\frac{g}{f\rho_0}(z+\frac{h}{2})\nabla\rho\,, \qquad (28)$$

which is a simplification of (14). This velocity profile is applied in addition to the prognostic velocities. It has no net mass transport, and to the extent that the thermodynamic variables are vertically well mixed it may contribute a negligible lateral heat or salt transport, even though it may enter prominently into the mixed layer TKE budget.

This placeholder parameterization is not entirely satisfactory in some regards. Unless it substantially controls the horizontal density gradients even at well-resolved scales, (28) would not be independent of resolution. Also, there is no particular reason why the optimal viscous mixing should be a good proxy for the small-scale straining of horizontal density gradients. Still it is at least a parameterization with a plausible magnitude for assessing whether viscous restratification could be significant in determining the ocean's mixed-layer depth.

As shown in Figs. 11 and 12, this parameterization of shear driven restratification has a dramatic impact on the mixed-layer depth. The zonal mean mixed-layer depth with the parameterization is roughly 60% of the depth without the parameterization, with a particularly substantial reduction in the mixed-layer depth in the Southern Ocean. With the parameterization, the resolved jets are sites of substantial subduction, with relatively shallow mixed-layer depths. The plausible magnitude (but not necessarily accurate) parameterization considered here indicates that viscous restratification is an important process for further study. The interaction between horizontal and column processes may offer prospects for improvements to climate models that are at least as important as improvements to the representation of column mixed layer physics.

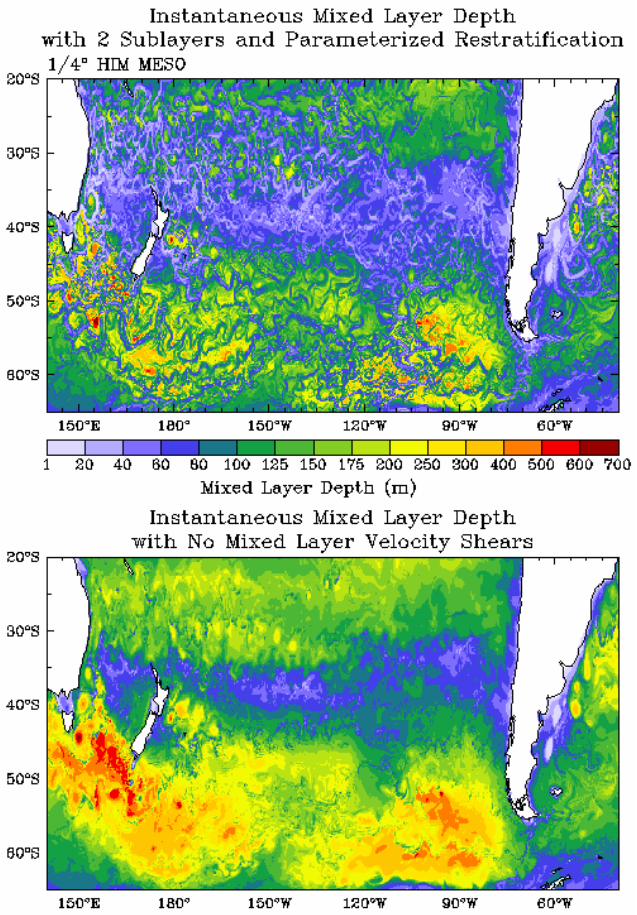

Figure 12. Instantaneous mixed-layer depths in an eddy-permitting (1/4 degree Mercator resolution) simulation of the Southern Hemisphere circulation. These simulations are a part of the "Modeling Eddies in the Southern Ocean" (MESO) project (*Hallberg et al.*, 2003). The top panel includes both two sublayers in the mixed layer and a direct parameterization of shear driven restratification, while the lower panel enforces a constant velocity through the mixed layer. The case in the bottom was started from the one on top, and has been run for just 100 days. Without a seasonal cycle in the forcing, the mixed-layer depth grows gradually without bound in the lower case. The depths in the top panel are much more reasonable, but direct comparison with observations is ambiguous in the absence of a seasonal cycle. The streaks of relatively shallow mixed-layer depth in the top panel coincide with surface jets.

Conclusions

The two substantial barriers to improving the representation of boundary mixing processes in large-scale ocean models are a resolution that is consistent with the parameterization, and numerical techniques that are sufficiently accurate that the parameterized processes dominate numerical errors.

Models must resolve the scales upon which parameterizations are based and over which parameterizations act. This seemingly obvious point is illustrated with several examples drawn from the representation of entraining gravity currents and in representing the surface mixed layer. In each case, the resolution is distinct from the parameterization itself, but the resolution is necessary for the parameterization to be applied.

The numerical techniques currently in use are reasonably adiabatic in eddy-free ocean models with appropriate parameter settings, but may lead to levels of diapycnal diffusion that greatly exceed physically justifiable levels in eddy-rich Z- or σ-coordinate ocean model simulations. Ironically, the two barriers to introducing improved representations of physical mixing conflict. Increasing resolution to accommodate parameterizations may also lead to greater numerical watermass modifications that would mask the very parameterizations being introduced! This conflict is quite likely the greatest barrier to improving the physical consistency of the representation of mixing in large-scale ocean models.

Although isopycnic coordinate models naturally avoid much of the spurious watermass modifications that plague other models, even at eddy-permitting resolutions. There remain hurdles to the use of such models for large-scale climate simulations, especially in the formulation of the surface mixed layer and its interaction with horizontal and interior processes.

The refined bulk mixed layer, described here in some detail, provides an avenue for admitting horizontal influences on the mixed-layer depth. These are excluded by construction from traditional bulk mixed-layer models and may be a large part of the reason why bulk mixed layers are not viewed as favorably as are diffusivity profile-based parameterizations. The refined bulk mixed layer permits either the direct representation (at high enough resolution) or the parameterization of viscous restratification. The impact of viscous restratification on the mixed-layer depth has yet to be fully understood, but a plausible parameterization is shown here to have a dramatic impact on the mixed-layer depth in an eddy-permitting Southern Hemisphere simulation.

The path to developing large-scale ocean models that more accurately represent boundary mixing processes and their interactions with the ocean circulation will not be easy. It is an endeavor that will require close collaborations between oceanic observations, process studies, and large-scale model numerical developments. But as the hurdles along the way are increasingly recognized, there is the strong prospect that such an effort will be fruitful in reducing the uncertainties in predictions of the ocean's behavior in a changing global climate system.

Acknowledgments. I wish to thank Anand Gnanadesikan for the use of some of his unpublished mixed layer data and insights, and Steve Griffies for extensive discussions of this subject. Both are also gratefully acknowledged for their internal reviews of this manuscript. In addition, I would like to thank the 'Aha Huliko'a coordinators for organizing a delightfully instructive workshop.

References

Bleck, R., An oceanic general circulation model framed in hybrid isopycnic-Cartesian coordinates, *Ocean Mod.*, *4*, 55-88, 2002.

Bleck, R., H. P. Hansen, D. Hu, and E. B. Kraus, Mixed layer-thermocline interaction in a three-dimensional isopycnic coordinate model, *J. Phys. Oceanogr.*, *19*, 1417-1439, 1989.

Bryan, K., and L. J. Lewis, A water mass model of the world ocean. *J. Geophys. Res.*, *84*, 2503-2517, 1979.

Chen, D., L. M. Rothstein, and A. J. Busalacchi, A hybrid vertical mixing scheme and its application to tropical ocean models, *J. Phys. Oceanogr*., *24*, 2156-2179, 1994.

Ellison, T. H., and J. S. Turner, Turbulent entrainment in stratified flows, *J. Fluid Mech.*, *6*, 423-448, 1959.

Ferrari, R., and D. L. Rudnick, Thermohaline variability in the upper ocean, *J. Geophys. Res*., *105*, 16857-16883, 2000.

Ferrari, R., and W. R. Young, On the development of thermohaline correlations as a result of nonlinear diffusive parameterizations, *J. Marine Res.*, *55*, 1069-1101, 1997.

Galbraith, N.R., A. Gnanadesikan, W.M. Ostrom, E.A. Terray, B.S. Way, N.J. Williams, S.H. Hill, and E. Terrill, 1996: Meteorological and oceanographic data during the ASREX III Field Experiment: Cruise and Data Report, *Woods Hole Oceanographic Inst. Tech.*

Rep 96-10, 247 pp, 1996.

Gaspar, P., Modeling the seasonal cycle of the upper ocean, *J. Phys. Oceanogr*., *18*, 161-180, 1988.

Gent., P. R., and J. C. McWilliams, Isopycnal mixing in ocean circulation models, *J. Phys. Oceanogr*., *20*, 150-155, 1990.

Gregg, M., Variations in the intensity of small-scale mixing in the main thermocline, *J. Phys. Oceanogr*., *7*, 436-454, 1977.

Griffies, S. M., The Gent-McWilliams skew flux, *J. Phys. Oceanogr.*, *28*, 831-841, 1998.

Griffies, S. M., A. Gnanadesikan, R. C. Pacanowski, V. Larichev, J. K. Dukowicz, and R. D. Smith, Isoneutral diffusion in a Z-coordinate ocean model, *J. Phys. Oceanogr.*, *28*, 831-841, 1998.

Griffies, S. M., R. C. Pacanowski, and R. W. Hallberg, Spurious diapycnal mixing associated with advection in a Z-coordinate ocean model. *Mon. Wea. Rev*., *128*, 538-564, 2000.

Hallberg, R., and P. B. Rhines, Buoyancy-driven circulation in an ocean basin with isopycnals intersecting the sloping boundary, *J. Phys. Oceanogr.*, *26*, 913-940. 1996.

Hallberg, R., Time integration of diapycnal diffusion and Richardson number-dependent mixing in isopycnal coordinate ocean models, *Mon. Wea. Rev.*, *128*, 1402-1419, 2000.

Hallberg, R., A. Gnanadesikan, S. M. Griffies, B. L. Samuels, J. R. Toggweiler, and G. K. Vallis, Southern Ocean eddies and the global overturning circulation: Initial results from "Modeling Eddies in the Southern Ocean (MESO)", in preparation, 2003.

Killworth, P. D. and N.R. Edwards, A turbulent bottom boundary layer code for use in numerical ocean models, *J. Phys. Oceanogr*., *29*, 1221-1238, 1999.

Large, W. G., J. C. McWilliams, and S. C. Doney, Oceanic vertical mixing: A review and a model with a nonlocal boundary layer parameterization, *Rev. Geophys.*, *32*, 363-403, 1994.

Lee, M.-M., A. C. Coward, and A. J. G. Nurser, Spurious diapycnal mixing of the deep waters in an eddy-permitting global ocean model, *J. Phys. Oceanogr*., *32*, 1552-1535, 2002.

Murtugudde, R., M. Cane, and V. Prasad, A reduced-gravity, primitive equation, isopycnal ocean GCM: formulation and simulations, *Mon. Wea. Rev.*, *123*, 2864-2887, 1995.

Oberhuber, J. M., Simulation of the Atlantic circulation with a coupled sea ice - mixed layer – isopycnal general circulation model. Part I: Model description. *J. Phys. Oceanogr*., *23*, 808-829, 1993.

Özgökmen, T.M., and E.P. Chassignet, Dynamics of two-dimensional turbulent bottom gravity currents. *J. Phys. Oceanogr.*, *32*, 1460-1478, 2002.

Niiler, P. P. and E. B. Kraus, One-dimensional models of the upper ocean thermocline. *Modelling and Prediction of the Upper Layers of the Ocean.* E. B. Kraus, Ed., Pergamon Press, 143-172, 1977.

Nurser, A. J. G., and J. F. Zhang, Eddy-induced mixed layer shallowing and mixed layer/thermocline exchange *J. Geophys. Res*., *105*, 21851-21868, 2000.

Papadakis, M. P., E. P. Chassignet, and R. W. Hallberg, Numerical simulations of the Mediterranean sea outflow: impact of the entrainment parameterization in an isopycnic coordinate ocean model, *Ocean Mod.*, *5*, 325-356, 2003.

Pollard, R. T., P. B. Rhines, and R. O. R. Y. Thompson, The deepening of the wind-mixed layer, *Geophys. Fluid Dyn.*, *4*, 381-404, 1973.

Polzin, K. L., J. M Toole, J.R. Ledwell, and R. W. Schmitt, Spatial variability of turbulent mixing in the abyssal ocean, *Science*, *276*, 93-96. 1997.

Price, J. F., and M. O. Baringer, Overflows and deep water production by marginal seas, *Prog. Oceanogr.*, *33*, 161-200, 1994.

Price, J. F., R. A. Weller, and R. Pinkel, Diurnal cycling: observations and models of the upper ocean response to diurnal heating, cooling, and wind mixing. *J. Geophys. Res.*, *91*, 8411-8427, 1986.

Redi, M. H., Oceanic isopycnal mixing by coordinate rotation, *J. Phys. Oceanogr*., *12*, 1154-1158, 1982.

Roberts, M., and D. Marshall, Do we require adiabatic dissipation schemes in eddy-resolving ocean models? *J. Phys. Oceanogr*., *28*, 2050-2063, 1998.

Rodhe, J., Wind mixing in a turbulent surface layer in the presence of a horizontal density gradient, *J. Phys. Oceanogr*., *21*, 1080-1083, 1991.

Rudnick, D. L. and R. Ferrari, Compensation of horizontal temperature and salinity gradients in the ocean mixed layer, *Science*, *283*, 526-529. 1999.

Simmons, H. L., S. R. Jayne, L. C. St. Laurent and A. J. Weaver, Tidally driven mixing in a numerical model of the ocean general circulation, *Ocean Mod.*, in press, 2003.

Solomon, H., On the representation of isentropic mixing in ocean circulation models, *J. Phys. Oceanogr*., *1*, 1032-1035, 1971.

Thompson, L., K. Kelly, D. Darr, and R. Hallberg, Buoyancy and mixed layer effects on the sea surface height response in an isopycnal model of the North Pacific Wind mixing in a turbulent surface layer in the presence of a horizontal density gradient, *J. Phys. Oceanogr*., *32*, 3657-3670, 2002.

Veronis, G., The use of tracers in circulation studies. *The*

Sea, E. D. Goldberg et al., Eds., Vol. 6, Wiley Inter-Science, 169-188, 1977.

Weller, R. A., Overview of the Frontal Air-Sea Interaction Experiment (FASINEX), *J. Geophys. Res*., *96*, 8501-8516, 1991.

Winton, M., R. Hallberg, and A. Gnanadesikan, Simulation of density-driven frictional downslope flow in Z-coordinate models. *J. Phys. Oceanogr*., *28*, 2163-2174, 1998.

Young, W., The subinertial mixed layer approximation, *J. Phys. Oceanogr*., *24*, 1812-1826, 1994.